Ward identity of the vector current and the decay rate of $\eta_c \to \gamma\gamma$ in lattice QCD

Chuan Liu,[1,2] Yu Meng,[1,*] and Ke-Long Zhang[1]

[1]*School of Physics and Center for High Energy Physics, Peking University, Beijing 100871, P.R. China*
[2]*Collaborative Innovation Center of Quantum Matter, Beijing 100871, P.R. China*

(Received 14 April 2020; accepted 23 July 2020; published 5 August 2020)

Using a recently proposed method [Y. Meng, C. Liu, and K. L. Zhang, arXiv:1910.11597v3], we study the two-photon decay rate of η_c using two $N_f = 2$ twisted mass gauge ensembles with lattice spacings 0.067 fm and 0.085 fm. The results obtained from these two ensembles can be extrapolated in a naive fashion to the continuum limit, yielding a result that is consistent with the experimental one within two standard deviations. To be specific, we obtain the results for two-photon decay of η_c as $\mathcal{B}(\eta_c \to 2\gamma) = 1.29(3)(18) \times 10^{-4}$ where the first error is statistical and the second is our estimate for the systematic error caused by the finite lattice spacing. It turns out that Ward identity for the vector current is of vital importance within this new method. We verify that the Ward identity is violated for local current with a finite lattice spacing, however it will be restored after the continuum limit is taken.

DOI: 10.1103/PhysRevD.102.034502

I. INTRODUCTION

The charmonium two-photon decay process $\eta_c \to 2\gamma$ has long been an ideal testing ground for the understanding of nonperturbative nature of quantum chromodynamics (QCD) [1] due to the medium energy scale of charmonium systems in strong interactions [2]. On one hand, it offers an access to the strong coupling constant at the charmonium scale within the framework of perturbative QCD. On the other hand, it also provides a sensitive test for the application of effective field theories such as nonrelativistic QCD (NRQCD) [3], which plays an important role in the treatment of quarkonium spectrum, decay and production. For the reasons given above, this question has been addressed extensively in the literature from both experiments [4–7] and various theoretical methods, notably NRQCD and lattice QCD studies [8–11].

Combining the experimental results in recent years, the latest Particle Data Group (PDG) lists the branching fraction for this process as $\mathcal{B}(\eta_c \to 2\gamma) = (1.57 \pm 0.12) \times 10^{-4}$ [12]. Despite the significant effort on the theoretical side over the years, the progress has been slow so far. Namely, none of the existing results come even close to the experimental values, to the best of our knowledge. For example, within the framework of NRQCD factorization, the authors in Ref. [11] have computed the next-to-next-to-leading order QCD corrections to this process, yielding a value for $\mathcal{B}(\eta_c \to 2\gamma)$ that is about twice the one quoted by PDG. In some sense, this discrepancy might indicate that NRQCD breaks down for such processes due to substantial nonperturbative effects.

It is then natural to turn to genuine nonperturbative methods such as lattice QCD (LQCD). With the proposal and realization of photon hadronic structure on lattice in Refs. [13], such an idea has been widely applied to photon structure functions [14], radiative transition [15], two-photon decays in charmonia [8–10], and neutral pion two-photon decay [16]. The first quenched LQCD calculation of $\eta_c \to 2\gamma$ was presented in 2006 [8] and unquenched results followed in recent years [9,10]. All these available lattice results have been summarized in Table I as well. As a comparison, we also list the results of NRQCD and the PDG value. It is evident that none of these existing theoretical results can explain the PDG value satisfactorily so far.

In previous lattice calculations of charmonia double gamma decay, the relevant hadronic matrix elements are decomposed into form factors which are functions of photon virtualities $Q_i^2, i = 1, 2$. Via an appropriate fitting of matrix element at different Q_i^2 with a specific functional form, one obtains the complete off-shell form factors. Then, the physical decay width can be obtained by setting all virtualities to the on-shell values, namely $Q_i^2 = 0$, yielding the final decay rate. However, the large deviations between the experiments and lattice results in Refs. [8–10] indicate that such methods might suffer from rather severe lattice

*mengyu1905@gmail.com

TABLE I. Results of $\mathcal{B}(\eta_c \to 2\gamma)$ obtained with different theoretical methods. The uncertainties in the table include both the statistical and systematic errors added in quadrature whenever available. The latest Particle Data Group (PDG) result is also given for comparison.

Methods	Value $\times 10^{-4}$	Uncertainty $\times 10^{-4}$	References
Quenched Wilson	0.83	0.50	[8]
$N_f = 2$ twisted mass	0.351	0.004	[9]
NRQCD	$3.1 \sim 3.2$		[11]
PDG	1.57	0.12	[12]

artifacts and the decomposition itself might also be troublesome on the lattice with finite lattice spacings. This is understandable in a way since, for such processes, the photons in the final state are rather energetic (typically 1.5 GeV in physical unit) in lattice units for commonly used lattice spacings.

Therefore, it is of great significance to explore new lattice methods. In a recent work [17], we have proposed a new method to compute the three-photon decay rate of J/ψ on the lattice directly with all polarizations of the initial and final states summed over. Such a method is originally put forward to avoid the complicated decomposition of the matrix element $M(J/\psi \to 3\gamma)$. In this paper, we would apply this new method to two-photon decay of η_c, which is in fact the simplest case that one could imagine. If we are only interested in the physical decay width, i.e., on-shell matrix elements, we can simply sum over all polarizations of the initial and final particles. It should be emphasized that the Ward identities associated with the vector currents are crucial for this summation process. In the continuum Minkowski space, the summation over photon polarizations always yields the Minkowski metric, e.g., $\sum_{\lambda_i}(\epsilon_{\mu}^{\lambda_i}(q_i)\epsilon_{\mu'}^{\lambda_i,*}(q_i) \Rightarrow -g_{\mu\mu'}$ due to Ward identities. Generally speaking, Ward identity is broken for a finite lattice spacing a. Hence, one has to consider the so-called Ward identity breaking (WIB) corrections when summing over the photon polarizations on lattice. Nevertheless, as we will see below, one can still stick to this substitution as long as the summation over all polarizations of initial and final particles is performed. This comes from the fact that the WIB effects for on-shell matrix element eventually vanish after taking the continuum limit $a \to 0$.

The rest of this paper is organized as follows. In Sec. II, we give a detailed derivation of the matrix element for the case of two-photon decay of η_c. In Sec. III, we compare the new method that has been proposed in Ref. [17] with the conventional approaches and explain how the decay width can be obtained directly without the decomposition of the relevant form factor. In Sec. IV, details of simulations are provided and the main results are presented. This section is divided into three parts: in Sec. IV A, the lattice dispersion relation for η_c is checked; in Sec. IV B, the current renormalization constant is calculated; in Sec. IV C, numerical results of the matrix element squared and the corresponding WIB corrections are provided. These results are eventually converted into the two-photon decay width of η_c. A naive continuum extrapolation is then performed and the final results are compared with the PDG value. It is found that our result is consistent with the PDG value within two standard deviations. Finally, we conclude in Sec. V.

II. APPROACH TO DECAY AMPLITUDE ON LATTICE

In this section, we recapitulate on the general method utilized in previous lattice studies on the two-photon decay width of η_c [8–10]. We start by expressing the decay matrix element of $\eta_c \to 2\gamma$ in terms of the appropriate three-point function using Lehmann-Symanzik-Zimmermann reduction formula in Minkoswki space and integrating out the photon fields perturbatively. It then follows that the relevant matrix element reads

$$\begin{aligned} M &= \langle \gamma(q_1,\lambda_1)\gamma(q_2,\lambda_2)|\eta_c(p)\rangle \\ &= \int d^4x \int d^4y \mathcal{H}_{\mu\nu}(x,y)\mathcal{Q}^{\mu\nu}(x,y), \end{aligned} \tag{1}$$

where the two functions $\mathcal{H}_{\mu\nu}(x,y)$ and $\mathcal{Q}^{\mu\nu}(x,y)$, which will be called the hadronic and the nonhadronic part of the matrix element respectively, will be defined shortly. For later convenience, we reverse the operator time ordering and the decay amplitude M on finite lattice can be written as

$$M = \frac{1}{V \cdot T} \int d^4x \int d^4y \mathcal{H}_{\mu\nu}(x,y)\mathcal{Q}^{\mu\nu}(x,y) \tag{2}$$

where $V = L^3$, L is the space length and T is time length of the lattice. The factor $V \cdot T$ arises from the four-momentum conservation δ-function in a finite space-time volume. In the following, we will fix the meson at time slice t_f, and denote the first photon with four-momentum $q_1 = (\omega_1, \boldsymbol{q}_1)$ at time slice t_i and the other one at time slice t with four-momentum $q_2 = (\omega_2, \boldsymbol{q}_2)$.

A. The hadronic part $\mathcal{H}_{\mu\nu}$

The hadronic part of the matrix element, namely $\mathcal{H}_{\mu\nu}(x,y)$, is explicitly defined as

$$\mathcal{H}_{\mu\nu}(x,y) = \langle \eta_c(p)|T\{j_\nu(y)j_\mu(x)\}|0\rangle, \tag{3}$$

where $|0\rangle$ and $|\eta_c(p)\rangle$ stands for the QCD vacuum state and the state with a single η_c meson with four-momentum p, respectively. The conserved vector current operator $j_\mu(x) = \bar{q}_f(x)\gamma_\mu q_f(x)$ comes in for various quark flavors f with $f = u, d, s, c$. However, if we were to consider only the

connected contributions, only the charm quark contribution (i.e., $f = c$) needs to be taken into account. To produce the meson η_c with three-momentum $\boldsymbol{p}$ from the QCD vacuum, we introduce the interpolating field operator $\hat{\mathcal{O}}_{\eta_c}(\boldsymbol{z}, t_f)$ in coordinate space that carries the quantum number of η_c,

$$|\eta_c(p)\rangle = \sum_{\boldsymbol{z}} e^{i\boldsymbol{p}\cdot\boldsymbol{z}} \hat{\mathcal{O}}_{\eta_c}(\boldsymbol{z}, t_f)|0\rangle. \tag{4}$$

We can substitute this into Eq. (3) and insert the following completeness relation

$$\mathbf{1} = \frac{1}{V}\sum_{n,\boldsymbol{p}} \frac{1}{2E_n(\boldsymbol{p})} |n,\boldsymbol{p}\rangle\langle n,\boldsymbol{p}|, \tag{5}$$

where $|n,\boldsymbol{p}\rangle$ stands for the eigenstate of QCD Hamiltonian. Here $\boldsymbol{p}$ indicates the meson three-momentum and n the corresponding energy level. For large enough t_f, the ground state with $n = 0$ dominates the resulting expression. For simplicity, we denote $E_0(\boldsymbol{p})$ as $E_{\boldsymbol{p}}$ and the final expression for the hadronic part $\mathcal{H}_{\mu\nu}(x, y)$ reads,

$$\mathcal{H}_{\mu\nu}(x,y) = \sum_{t_f\to-\infty} \frac{2E_{\boldsymbol{p}}}{Z_{\eta_c}(\boldsymbol{p})} e^{E_{\boldsymbol{p}} t_f} \times \left\langle 0 \middle| T\left\{ \sum_{\boldsymbol{z}} e^{-i\boldsymbol{p}\cdot\boldsymbol{z}} \hat{\mathcal{O}}_{\eta_c}(\boldsymbol{z}, t_f) j_\nu(y) j_\mu(x) \right\} \middle| 0 \right\rangle, \tag{6}$$

with $Z_{\eta_c}(\boldsymbol{p})$ being the ground state amplitude $\langle\eta_c(\boldsymbol{p})|\hat{\mathcal{O}}_{\eta_c}(0)|0\rangle$.

B. The nonhadronic part $\mathcal{Q}^{\mu\nu}$

Similarly, the nonhadronic, or to be more precise, the photonic part is given by

$$\mathcal{Q}^{\mu\nu}(x,y) = -\lim_{\substack{q_1'\to q_1 \\ q_2'\to q_2}} e^2 q_1'^2 q_2'^2 \epsilon^{\lambda_1}_{\mu'}(q_1)\epsilon^{\lambda_2}_{\nu'}(q_2) \int d^4w \int d^4v \times e^{-iq_1'\cdot w - iq_2'\cdot v} D^{\mu\mu'}(x,w) D^{\nu\nu'}(y,v), \tag{7}$$

where $\epsilon^{\lambda_i}_{\mu'}(q_i)$ denotes the photon polarization vector with arbitrary four-momentum q_i and helicity λ_i. It can be obtained by an appropriate Lorentz transformation from the standard basis $\epsilon^1_{\mu'} = (0,1,0,0)$ and $\epsilon^2_{\mu'} = (0,0,1,0)$. The free photon propagator $D^{\mu\mu'}(x,w)$ is given by

$$D^{\mu\mu'}(x,w) = -ig^{\mu\mu'} \int \frac{d^4k}{(2\pi^4)} \frac{e^{-ik\cdot(x-w)}}{k^2 + i\epsilon}, \tag{8}$$

which cancels out the inverse propagator outside the integral in Eq. (7) in momentum space. As explained in Ref. [13], the resulting expression for $\mathcal{Q}_{\mu\nu}$ can then be analytically continued from Minkowski to Euclidean space. This process introduces the photon virtualities given by $Q_i^2 = |\boldsymbol{q}_i|^2 - \omega_i^2$, which are not too timelike to produce any on-shell vector hadrons. To be specific, one needs to ensure that $Q_i^2 = |\boldsymbol{q}_i|^2 - \omega_i^2 > -M_V^2$ where M_V is mass of the lightest vector meson in question. Assuming that the above conditions are satisfied and substituting the expression of the free photon propagator into Eq. (7), we finally obtain the following expression for $\mathcal{Q}^{\mu\nu}(x,y)$ in Euclidean space,

$$\mathcal{Q}^{\mu\nu}(x,y) = e^2 \epsilon^{\lambda_1}_{\mu}(q_1)\epsilon^{\lambda_2}_{\nu}(q_2) e^{-\omega_1 t_i - \omega_2 t} e^{i\boldsymbol{q}_1\cdot\boldsymbol{x} + i\boldsymbol{q}_2\cdot\boldsymbol{y}} \tag{9}$$

where the standard Wick rotation $t_i \to -it_i$, $t \to -it$ has been carried out.

Combining the results in Eqs. (2), (6), and (9), the final result of the matrix element then has the form as $M \sim \frac{1}{T}\int dt \int dt_i (\cdots)$. In real lattice simulations, the integral over the time slices t_i and t are replaced by discrete summations. For quantities that develops plateau behaviors in t, which is the case in our study, this second summation average can be replaced by its corresponding pleateau value. Eventually, the decay amplitude can be written as

$$M(t,t_i) = \lim_{t_f - t\to\infty} e^2 \frac{\epsilon^{\lambda_1}_{\mu}(q_1)\epsilon^{\lambda_2}_{\nu}(q_2)}{\frac{V\cdot Z_{\eta_c}(\boldsymbol{p})}{2E_{\eta_c}(\boldsymbol{p})} e^{-E_{\eta_c}(\boldsymbol{p})(t_f - t)}} \int dt_i e^{-\omega_1|t_i - t|} \times \left\langle 0 \middle| T\left\{ \sum_{\boldsymbol{z}} e^{-i\boldsymbol{p}\cdot\boldsymbol{z}} \hat{\mathcal{O}}_{\eta_c}(\boldsymbol{z}, t_f) \int d^3\boldsymbol{y} e^{i\boldsymbol{q}_2\cdot\boldsymbol{y}} j_\nu(\boldsymbol{y}, t) \int d^3\boldsymbol{x} e^{i\boldsymbol{q}_1\cdot\boldsymbol{x}} j_\mu(\boldsymbol{x}, t_i) \right\} \middle| 0 \right\rangle. \tag{10}$$

The correlation function appearing in above equation can be calculated by lattice QCD in terms of quark propagators. In the following, we denote the matrix element in Eq. (10) as $M = \epsilon_\mu \epsilon_\nu \mathcal{M}_{\mu\nu}$. Each $\mathcal{M}_{\mu\nu}$ can be computed on the lattice by searching for a plateau behavior in t, as long as $t_f - t$ is large enough. In principle, the current operators in

above equation contain all flavors of quarks weighted by their corresponding charges. However, since the light quarks can only enter the question by disconnected diagrams which are ignored in this study. In this simulation, the local current $j_\mu(x) = \bar{c}(x)\gamma_\mu c(x)$ is adopted for the charm quark which can be renormalized by a multiplicative factor Z_V. The integrals of t_i in Eq. (10) are also replaced by corresponding trapezoidal summation. Note that it is usually impossible to exactly put both photons with discrete momenta q_i on shell because of the energy-momentum conservation, hence the matrix element $\mathcal{M}_{\mu\nu}$ calculated on the lattice is always slightly off-shell with some nonvanishing photon virtualities $Q_i^2, i = 1, 2$.

III. NEW APPROACH TO THE DECAY WIDTH ON THE LATTICE

In this section, we first discuss the relationship between amplitude M and decay width Γ with conventional method [8–10], and then introduce the new method that has been put forward in Ref. [17].

In conventional simulations, the matrix element $\mathcal{M}_{\mu\nu}$ is parametrized in terms of a form factor $F(Q_1^2, Q_2^2)$ as,

$$\mathcal{M}_{\mu\nu} = 2\left(\frac{2}{3}e\right)^2 m_{\eta_c}^{-1} F(Q_1^2, Q_2^2)\epsilon_{\mu\nu\rho\alpha}q_1^\rho q_2^\sigma. \tag{11}$$

The physical on-shell decay width Γ for η_c decaying to two physical photons is related to the form factor at $Q_1^2 = Q_2^2 = 0$,

$$\Gamma = \pi\alpha_{em}^2\left(\frac{16}{81}\right)m_{\eta_c}|F(0,0)|^2, \tag{12}$$

where $\alpha_{em} \simeq (1/137)$ is the fine structure constant in quantum electrodynamics (QED). Such decomposition is valid under the assumption of full Lorentz invariance and Bose symmetry. However, when evaluated on a hypercubic lattice with finite lattice spacing, the matrix element $\mathcal{M}_{\mu\nu}$ has less symmetry. Strictly speaking, this decomposition can only be utilized only when the relevant momenta, namely the components of q_1 and q_2, are small in lattice units. This might become problematic since the typical momentum of each photon in the final state is roughly $m_{\eta_c}/2$.

In this paper we proceed in another way as advocated in Ref. [17]. To this end, we define

$$\begin{aligned}\mathcal{T} \equiv |M|^2 &= \sum_{\lambda_1,\lambda_2}\sum_{\mu\nu}|\epsilon_\mu^{\lambda_1}(q_1)\epsilon_\nu^{\lambda_2}(q_2)\mathcal{M}_{\mu\nu}|^2 \\ &= \sum_{\mu\nu}|\mathcal{M}_{\mu\nu}|^2,\end{aligned} \tag{13}$$

which will be called the $\mathcal{T}$-function in the following. In the above equation, Ward identity of the vector currents has been utilized, i.e., the summation over photon polarizations yields the Minkowski metric, e.g.,

$$\sum_{\lambda_i}\epsilon_\mu^{\lambda_i}(q_i)\epsilon_{\mu'}^{\lambda_i,*}(q_i) \Rightarrow -g_{\mu\mu'}. \tag{14}$$

In actual simulations, all possible $|\mathcal{M}_{\mu\nu}|^2$'s are summed over. The physical decay width of $\eta_c \to 2\gamma$ in the center of mass frame can be expressed as

$$\begin{aligned}\Gamma(\eta_c \to 2\gamma) &= \frac{1}{2!}\frac{1}{2m_{\eta_c}}\int\frac{d^3\boldsymbol{q}_1}{(2\pi)^3 2\omega_1}\frac{d^3\boldsymbol{q}_2}{(2\pi)^3 2\omega_2} \\ &\quad\times(2\pi)^4\delta^4(p - q_1 - q_2)|M|^2 \\ &= \frac{1}{16\pi m_{\eta_c}}\mathcal{T}.\end{aligned} \tag{15}$$

In the last line, the $\mathcal{T}$-function needs to be on-shell for a physical decay width.

As we already mentioned above, due to the discreteness of the three-momenta on the lattice, it is impossible to exactly impose the on-shell condition for all final particles, making the on-shell quantity $\mathcal{T}$ not directly accessible on finite lattices. However, a counterpart of it with small nonvanishing virtualities can be computed directly on the lattice. We denote this as $\mathcal{T}(Q_1^2, Q_2^2)$. This differs from the on-shell $\mathcal{T}$-function only because of the fact that some of the photons are still off-shell. The on-shell quantity $\mathcal{T}(0,0)$ can be obtained by the following fitting formula,

$$\mathcal{T}(Q_1^2, Q_2^2) = \mathcal{T}(0,0) + \text{const} \times \sum_i Q_i^2 + \text{higher orders} \tag{16}$$

for $|Q_i^2| \ll 1$ where everything is measured in lattice units. We expect such behavior since the final two photons are identical.

Another issue is the breaking of the conventional Ward identities on the lattice. As we have seen, when performing the summation over polarizations of the photons, Ward identity plays a crucial role. On a finite lattice, however, Ward identity is usually violated. This is due to various reasons. First of all, the local vector current that we are using is not strictly conserved on the lattice. However, when renormalized by a multiplicative factor Z_V, it will be conserved in the continuum limit. Second, our photons are not strictly on-shell, represented by nonvanishing virtualities of the two photons. All of these will spoil the conventional Ward identity. The corresponding corrections to $\mathcal{T}$-function will be called Ward identity breaking (WIB) corrections in this paper. With WIB corrections included, the summation over polarizations of the photons should be modified as [18]

$$\sum_{\lambda_i}\epsilon_{\mu}^{\lambda_i}(q_i)\epsilon_{\mu'}^{\lambda_i,*}(q_i) \Rightarrow -g_{\mu\mu'}+\Delta_{\mu\mu'}^{(i)}, \tag{17}$$

where $\Delta_{\mu\mu'}^{(i)}=(q_\mu^i\bar{q}_{\mu'}^i+\bar{q}_\mu^i q_{\mu'}^i)/2\omega_i^2$ and $\bar{q}_\mu^i=(\omega_i,\boldsymbol{q}_i)$. Then, the $\mathcal{T}$-function with WIB corrections can be expressed as

$$\mathcal{T}(\Delta)=\mathcal{T}+\delta\mathcal{T}(\Delta), \tag{18}$$

where

$$\delta\mathcal{T}(\Delta)=(\Delta_{\mu\mu'}^{(1)}\Delta_{\nu\nu'}^{(2)}-g_{\nu\nu'}\Delta_{\mu\mu'}^{(1)}-g_{\mu\mu'}\Delta_{\nu\nu'}^{(2)})\mathcal{M}_{\mu\nu}\mathcal{M}_{\mu'\nu'}^{*} \tag{19}$$

represents the WIB correction term. In principle, one expects that $\delta\mathcal{T}(\Delta)$ approaches to zero in the continuum limit, which is also verified numerically in our simulations.

IV. SIMULATIONS AND RESULTS

Our simulations are performed using two $N_f=2$ flavor twisted mass gauge field ensembles generated by the Extended Twisted Mass Collaboration (ETMC) with lattice spacing $a\simeq 0.067$ fm and 0.085 fm, respectively. The corresponding physical pion masses are 300 MeV and 315 MeV. The most important advantage of these setups is so-called automatic $\mathcal{O}(a)$ improvement for the physical quantities with twisted mass quark action at maximal twist [19]. In Table II, we list all ensembles used in this study together with other relevant parameters.

For the valence sector, we employ the Osterwalder-Seiler setup where two extra twisted doublets are introduced, namely, (u,d) and (c,c') with twisted mass $a\mu_l$ and $a\mu_c$ [20–22]. For each doublet, the Wilson parameters have opposite signs ($r=-r'=1$). The quark fields in physical basis (q,q') are closely related to ones in twisted basis $(\chi_q,\chi_{q'})$, via an axial transformation, i.e.,

$$\begin{pmatrix} q \\ q' \end{pmatrix}=\exp(i\omega\gamma_5\tau_3/2)\begin{pmatrix} \chi_q \\ \chi_{q'} \end{pmatrix} \tag{20}$$

where ω is the twist angle, and $\omega=\pi/2$ corresponds to the maximal twist. In this simulation, we determine the heavy quark mass $a\mu_c$ by the physical η_c mass with the corresponding meson operator $\hat{\mathcal{O}}_{\eta_c}(z)=\bar{c}(z)\gamma_5 c(z)$ in physical basis and the explicit values are 0.2550 and 0.2018 for Ens.I and Ens.II, respectively.

TABLE II. Parameters for the gauge ensembles used in this study.

Ensemble	β	a(fm)	V/a^4	$a\mu_{\rm sea}$	m_π(MeV)	$N_{\rm conf}$
I	3.9	0.085	$24^3\times 48$	0.004	315	60
II	4.05	0.067	$32^3\times 64$	0.003	300	60

A. The dispersion relation of η_c

It is crucial to verify the discrete dispersion relation in Eq. (21) by calculating the energies of η_c at a series of three-momenta, since this particular discrete dispersion relation enters our simulations and is to be utilized to obtain the photon energy ω_i with given virtuality Q_i^2 (basically replacing m_{η_c} by iQ_i) and three momentum $\boldsymbol{q}_i$. The discrete dispersion relation for the meson η_c is

$$4\sinh^2\frac{E(\boldsymbol{p})}{2}=4\sinh^2\frac{m_{\eta_c}}{2}+Z_{\rm latt}\cdot 4\sum_i\sin^2\left(\frac{\boldsymbol{p}_i}{2}\right). \tag{21}$$

In Fig. 1, our results for the dispersion of η_c are shown for two ensembles. It is found that the constant $Z_{\rm latt}$ is almost 1, indicating that such discrete dispersion relation is well satisfied in our simulation. In this study, 4 sets of suitable momenta with corresponding virtualities Q_i^2 are chosen for the purpose of reaching an on-shell $\mathcal{T}$-function.

B. Z_V and $Z_{\eta_c}(\boldsymbol{p})$

To determinate current renormalization factor Z_V which is introduced to renormalize the photon current operator $j_\mu(x)=\bar{c}\gamma_\mu c(x)$, we calculate a ratio of the two-point function over the three-point function [15] as given by

$$Z_V^{(\mu)}(t)=\frac{p^\mu}{E_{\eta_c}(\boldsymbol{p})}\frac{\frac{1}{2}\Gamma^{(2)}_{\eta_c\eta_c}(\boldsymbol{p},t_f,t_i)}{\Gamma^{(3)}_{\eta_c\gamma_\mu\eta_c}(\boldsymbol{p},t_f,t,t_i)}, \tag{22}$$

where the factor $1/2$ accounts for the equal contribution to the two-point function of the source at time slice 0 and the image of the source at time slice T. For the particle in its

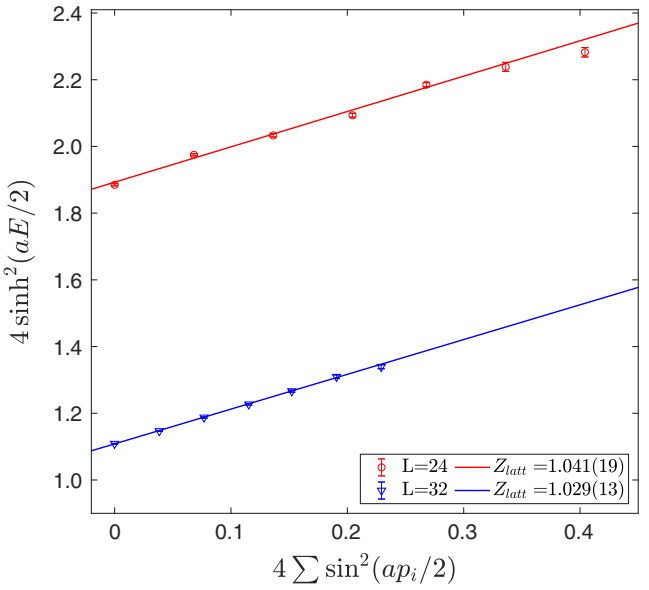

FIG. 1. The dispersion relation of meson η_c on two different volumes $L=24$(red) and $L=32$(blue), respectively.

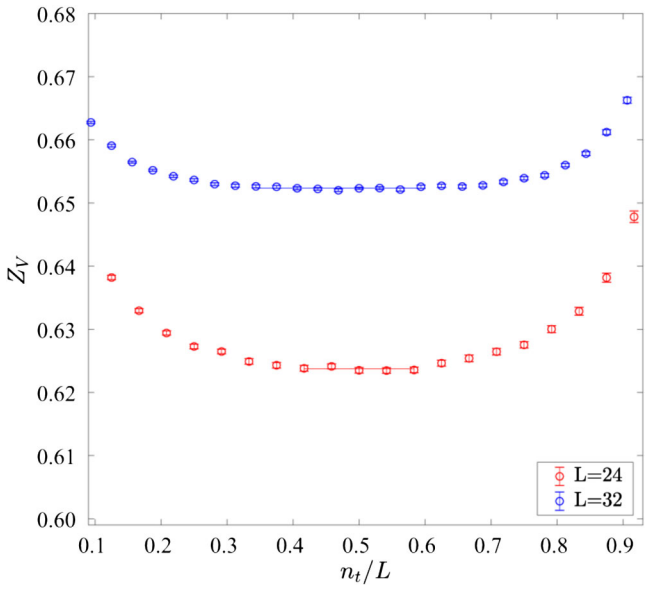

FIG. 2. The current renormalization constant $Z_V^{(\mu)}$ calculated by Eq. (22) for Ens.I (red points) and Ens.II (blue points), respectively.

rest frame, one has $\mu = 0$ and $\boldsymbol{p} = 0$. Thus, in the following, the index μ of $Z_V^{(\mu)}$ will be omitted. Therefore, the two-point function $\Gamma^{(2)}_{\eta_c\eta_c}$ and the three-point function $\Gamma^{(3)}_{\eta_c\gamma_\mu\eta_c}$ have such explicit forms as follows,

$$\Gamma^{(2)}_{\eta_c\eta_c} = \sum_{\boldsymbol{x},\boldsymbol{y}} \langle \mathcal{O}_{\eta_c}(\boldsymbol{x}, T/2)\mathcal{O}^{\dagger}_{\eta_c}(\boldsymbol{y}, 0)\rangle \tag{23}$$

$$\Gamma^{(3)}_{\eta_c\gamma_\mu\eta_c} = \sum_{\boldsymbol{x},\boldsymbol{y},z} \langle \mathcal{O}_{\eta_c}(\boldsymbol{x}, T/2)\bar{c}\gamma_\mu c(\boldsymbol{z}, t)\mathcal{O}^{\dagger}_{\eta_c}(\boldsymbol{y}, 0)\rangle. \tag{24}$$

where we have fixed $t_f = T/2$ and $t_i = 0$.

The plateau behavior of $Z_V^{(0)}(t)$ across different time slice t then yields the value of the renormalization factor Z_V. As an illustration, this is shown in Fig. 2 where the data points with errors are from our simulation and the horizontal bars indicate the intervals from which Z_V are extracted. The final values of Z_V are 0.6237(2), 0.6523(1) for $L = 24$ and $L = 32$, respectively.

The value of $Z_{\eta_c}(\boldsymbol{p})$ can be extracted directly from the two-point function,

$$\begin{aligned}\Gamma^{(2)}_{\eta_c\eta_c}(t) &= \sum_{\boldsymbol{x},\boldsymbol{y}} \langle \mathcal{O}_{\eta_c}(\boldsymbol{x}, t)\mathcal{O}^{\dagger}_{\eta_c}(\boldsymbol{y}, 0)\rangle \\ &\xrightarrow{t\gg 1} \frac{V\cdot|Z_{\eta_c}|^2}{E_{\eta_c}} e^{-E_{\eta_c}\frac{T}{2}} \cosh\left[E_{\eta_c}\left(\frac{T}{2} - t\right)\right]\end{aligned} \tag{25}$$

where $Z_{\eta_c} = Z_{\eta_c}(\boldsymbol{0})$, $E_{\eta_c} = E_{\eta_c}(\boldsymbol{0})$. In this simulation, the η_c meson is fixed at the time slice $t_f = T/2$ and the wall-source is adopted.

C. The decay width of $\eta_c \to 2\gamma$

The conventional sequential method has been adopted to calculate the three-point function in Eq. (10). We put the sequential source on one current with time slice t_i, and the contraction is performed on the other current at time slice t. After the integration (summation) of t_i, the matrix element $\mathcal{M}_{\mu\nu}$, being a function of t, can be obtained on the lattice.

The input parameters include photon momenta $\boldsymbol{q}_i = \frac{2\pi}{L}\boldsymbol{n}_i$, virtualities Q_i^2 and energies ω_i. For each set of photon momenta, a series of $\mathcal{M}_{\mu\nu}$ can be computed by varying Q_i^2. Such a strategy has been outlined in Refs. [8–10]. In fact, Q_2^2 is uniquely dependent on Q_1^2 due to energy-momentum conservation. In this simulation, we proceed in another way where two photons share the same virtualities $Q_1^2 = Q_2^2 = Q_m^2$, which is determined by

$$E_{\eta_c} = 4\ \sinh^{-1}\left(\sqrt{\sum_{i=1}^{3}\sin^2(\boldsymbol{q}^i/2) - \sinh^2(Q_m/2)}\right), \tag{26}$$

with $\boldsymbol{q} \equiv \boldsymbol{q}_1 = -\boldsymbol{q}_2$ and i being the spatial component index. For each set of momenta, we calculate 16 matrix elements $\mathcal{M}_{\mu\nu}$, including all polarizations of the two photons. In Fig. 3, typical plateau behaviors for the three-point function $\mathcal{M}_{\mu\nu}$ are shown in the case of $\mu = 1$, $\nu = 2$.

After the summation of 16 matrix elements $\mathcal{M}_{\mu\nu}$, the $\mathcal{T}$-function $\mathcal{T}(Q_m^2, t)$ can be obtained immediately and the results are shown in Fig. 4 for $\boldsymbol{n}_q = (0, 2, 2)$. The on-shell $\mathcal{T}$-function can be extracted by a fitting to Eq. (16) where two variables Q_1^2, Q_2^2 are utilized. In the case of Q_m^2, the on-shell fitting formula reduces to

$$\mathcal{T}(Q_m^2) = \mathcal{T}(0) + a \times Q_m^2 + b \times Q_m^4 \tag{27}$$

with $\mathcal{T}(0)$ and a and b being the fitting parameters. Ones can also include WIB terms and estimate its effect on the two-photon decay width of η_c. Note that the WIB effects only result from the nonconservation of the local current with a finite lattice spacing.

In the following, we denote $\mathcal{T}_W$ as the $\mathcal{T}$-function with WIB corrections included while $\mathcal{T}$ being the one without these corrections. Similar notations are applied for the decay widths Γ_W and Γ. Both the on-shell $\mathcal{T}_W$ and $\mathcal{T}$ under two spacings are shown in the left panel of Fig. 5 and the corresponding values are also summarized in Table III. Eventually, we obtain the two-photon decay widths of η_c for two ensembles with/without WIB corrections, respectively,

$$\begin{aligned}\Gamma^{(I)} &= 2.939(32)\ \text{keV}, \qquad \Gamma^{(I)}_W = 2.724(29)\ \text{keV} \\ \Gamma^{(II)} &= 3.404(27)\ \text{keV}, \qquad \Gamma^{(II)}_W = 3.228(25)\ \text{keV}\end{aligned} \tag{28}$$

The errors here only account for the statistical ones estimated by bootstrap method arising from the current renormalization

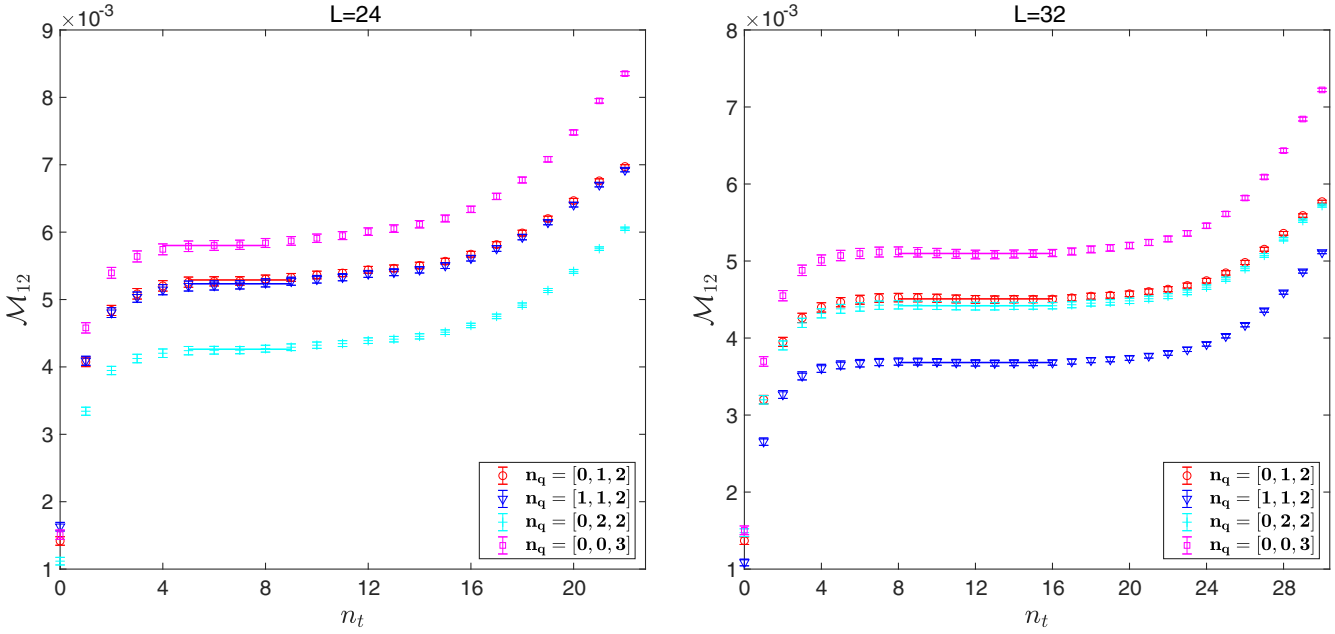

FIG. 3. The decay matrix elements $\mathcal{M}_{\mu\nu}$ obtained by summation over t_i for three-point function $\mathcal{M}_{\mu\nu}(t_i, t)$ with different volumes $L = 24$ (left) and $L = 32$ (right). As an example, only matrix elements with $\mu, \nu = 1, 2$ are shown under four different sets of photon momenta $\boldsymbol{n}_q$.

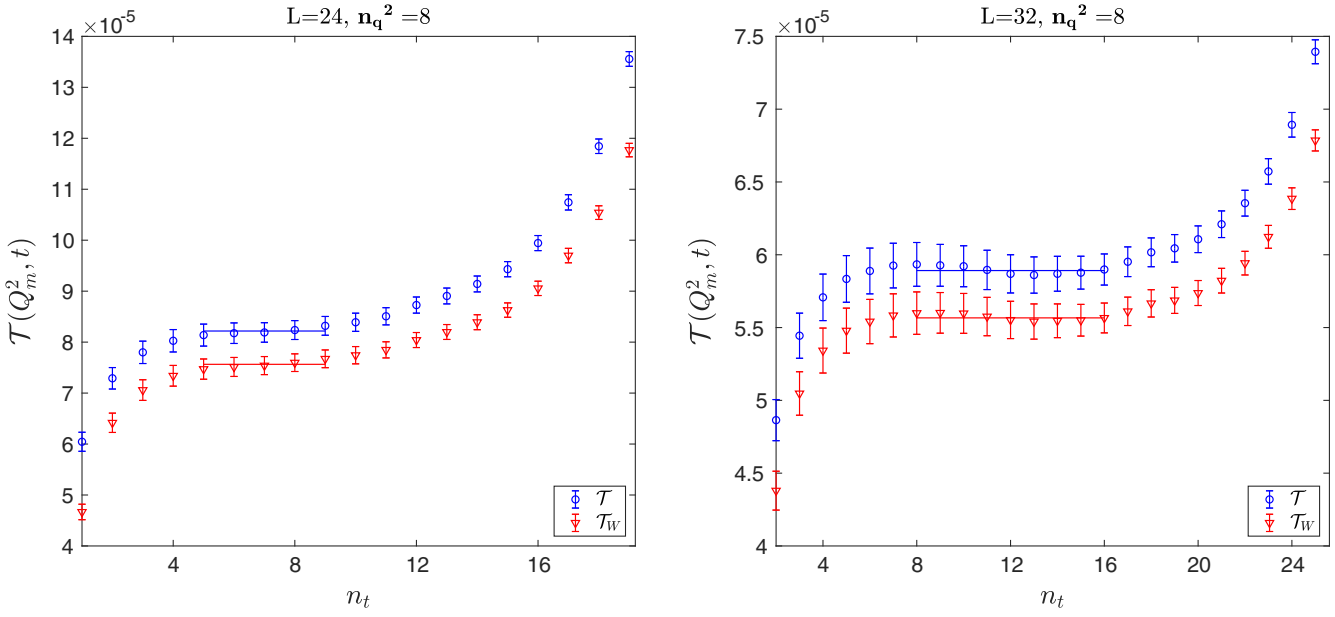

FIG. 4. The $\mathcal{T}$-function $\mathcal{T}(Q_m^2, t)$ as a function of t in case of photon momenta $\boldsymbol{n}_q = [0, 2, 2]$ and virtuality Q_m^2 under two different volumes $L = 24$ (left) and $L = 32$ (right), respectively. The red/blue data points correspond to $\mathcal{T}$-function with/without WIB corrections included given by the Eq. (19).

factor Z_V, ground state amplitude Z_{η_c} and on-shell fitting process as suggested in Eq. (27).

As seen from the results in Eq. (28), there exist discrepancies between Γ and Γ_W in both ensembles at finite lattice spacings. These differences can be viewed as an estimate of the finite lattice spacing error. Therefore, we take the difference between Γ and Γ_W as the estimate of the systematic error due to finite lattice spacings and the

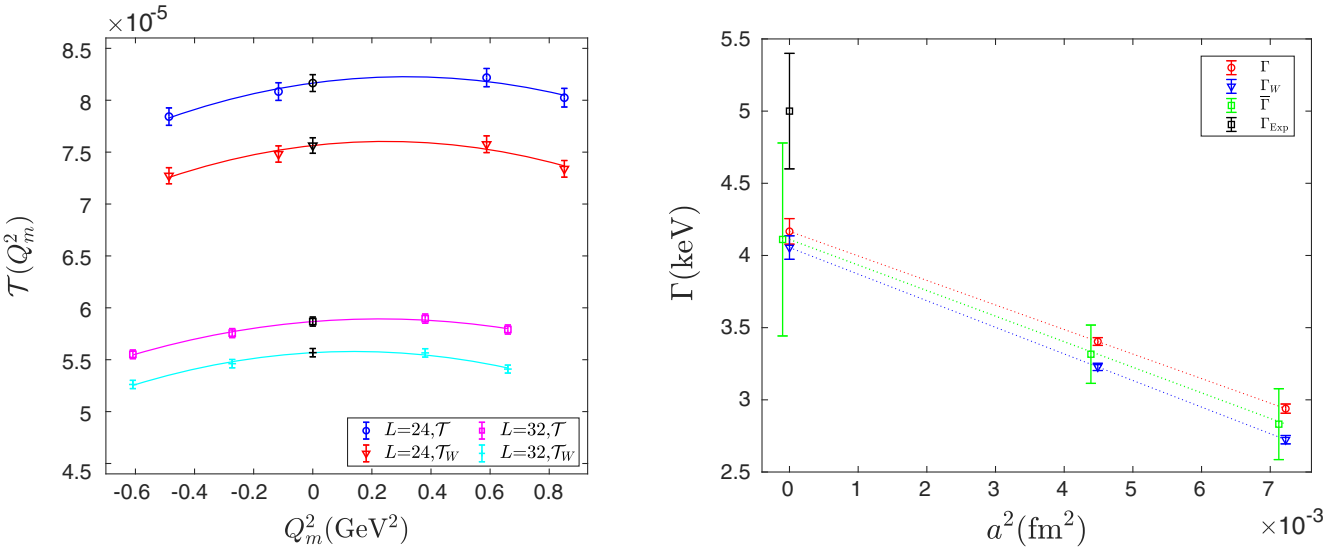

FIG. 5. Left panel: on-shell fitting for $\mathcal{T}$-function $\mathcal{T}(Q_m^2)$ and $\mathcal{T}_W(Q_m^2)$ under four sets of momenta for the two ensembles with $L = 24$, 32, respectively. The black points are the on-shell results fitted using Eq. (27) and other 4 colored points from left to right correspond to the momenta $\boldsymbol{n_q}^2 = 5$, 6, 8, 9; Right panel: a naive continuum extrapolation for two-photon decay width Γ, Γ_W and $\bar{\Gamma}$ under two different lattice spacings $a \simeq 0.067(\mathrm{fm}), 0.085(\mathrm{fm})$. The errors for $\bar{\Gamma}$ have included both statistical and estimated systematic errors. The green points of $\bar{\Gamma}$ have been shifted a bit horizontally to avoid overlap with other data points.

average of the two as the final decay width $\bar{\Gamma}$. Finally, we have

$$\bar{\Gamma}^{(I)} = 2.832(31)(215)\ \mathrm{keV}$$
$$\bar{\Gamma}^{(II)} = 3.316(26)(176)\ \mathrm{keV} \qquad (29)$$

where the first error is statistical and the second represents the estimate of the systematic error due to finite lattice spacing.

We now turn to a naive continuum extrapolation. For the study of charmonium with $N_f = 2$ configurations, one can assume an $\mathcal{O}(a^2)$ errors for the lattice results for the decay widths obtained above. This allows us to connect the two results for Γ, Γ_W, and $\bar{\Gamma}$ at two lattice spacings and obtain the corresponding results at $a = 0$. We call this the naive continuum extrapolation. since it is not a well-controlled continuum extrapolation. For that purpose, one needs at least three or more different lattice spacings. Taking the average of Γ and Γ_W, namely $\bar{\Gamma}$ as our final result, the decay width for the $\eta_c \to 2\gamma$ is found to be

$$\bar{\Gamma}(\eta_c \to 2\gamma) = 4.11(9)(58)\ \mathrm{keV}. \qquad (30)$$

TABLE III. $\mathcal{T}(0)$ without WIB corrections and $\mathcal{T}_W(0)$ with WIB corrections are fitted with Eq. (27).

	$\mathcal{T}(0) \times 10^{-5}$	χ^2/d.o.f	$\mathcal{T}_W(0) \times 10^{-5}$	χ^2/d.o.f
Ensemble I	8.165(82)	0.259	7.567(75)	0.057
Ensemble II	5.868(43)	0.242	5.565(42)	0.773

Here the first error is statistical and the second is the estimate of the systematic error due to finite lattice spacing.

These quantities are illustrated in Fig. 5. In the left panel, the on-shell fitting for $\mathcal{T}$ and $\mathcal{T}_W$ under two different spacings are performed. Obviously, the difference caused by the WIB effects is dependent on the lattice spacing, as expected. The finer the lattice spacing, the smaller the discrepancy. This is understandable since the breaking of the Ward identity is caused by finite lattice spacing. In the right panel of Fig. 5, we illustrate the naive continuum extrapolations for the decay width $\Gamma(\eta_c \to 2\gamma)$ and $\Gamma_W(\eta_c \to 2\gamma)$, respectively. In this limit, Γ and Γ_W are well consistent with each other as expected. Besides, the average of the $\Gamma(\eta_c \to 2\gamma)$ and $\Gamma_W(\eta_c \to 2\gamma)$, namely $\bar{\Gamma}$ is also shown. As is seen, with the finite lattice spacing errors included, the naive continuum extrapolated result is consistent with the experimental one within two standard deviations.

We emphasize that, all the continuum extrapolations, whether for Γ and Γ_W, or $\bar{\Gamma}$, are still preliminary due to the limited number of lattice spacings. Still, our final result for the decay width of $\eta_c \to 2\gamma$ is encouraging. This is the first lattice result which is consistent with the experiments within 2σ level. There are also other sources of systematic error: finite volume effects, pion mass which is still away from physical value and the contribution of disconnected diagrams. However, we think that finite lattice spacing errors are by far the most relevant one at present. Future lattice studies should aim to improve on this by utilizing more lattice ensembles which will substantially reduce this error.

The branching fraction, if the uncertainty of η_c total width ignored, is given by $\mathcal{B}(\eta_c \to 2\gamma) = 1.29(3)(18) \times 10^{-4}$,

where the first error is statistical and the second is our estimates for the systematics due to finite spacing. The result is consistent with the experiment result $\mathcal{B}_{\rm exp}(\eta_c \to 2\gamma) = 1.57(12) \times 10^{-4}$ [12] within two standard deviations. Compared to the previous much smaller ones obtained with traditional method of the form factor parametrizations, our results seem to indicate that the continuum form of parametrizations might fail drastically for the calculation of the hadronic decays on the lattice.

V. CONCLUSIONS

In this paper, we calculate the two-photon decay rate of η_c with all polarizations of the final photon states summed over, which is first proposed in Ref. [17]. Using two $N_f = 2$ twisted mass gauge ensembles with different lattice spacings, we have obtained the branching fraction $\mathcal{B}(\eta_c \to 2\gamma) = 1.29(3)(18) \times 10^{-4}$ where the first error is statistical and the second is our estimated systematic error due to finite lattice spacing. This result is consistent with the experimental one quoted by PDG within two standard deviations. An improved result would be expected in the future if more lattice spacings are utilized.

Furthermore, we have demonstrated that Ward identity for the current, which is essential for our method to work, is in fact violated with a finite lattice spacing a for a local current. After a detailed comparison between the decay width of $\eta_c \to 2\gamma$ with Ward identity breaking (WIB) effects included and excluded, we have shown that such a discrepancy vanishes in the continuum limit. This indicates that we can always replace the summation of photon polarizations safely by the Minkowski metric when we calculate the decay width of multiphoton final states as long as the continuum limit is taken in the end.

ACKNOWLEDGMENTS

The authors would like to thank Prof. Xu Feng at Peking University for helpful discussions. The authors also benefit a lot from inspiring discussions with the members of the CLQCD collaboration. The numerical works in this paper are obtained on "Era" petascale supercomputer of Computer Network Information Center of Chinese Academy of Science. This work is also supported in part by the National Science Foundation of China (NSFC) under the Project No. 11935017. It is also supported in part by the DFG and the NSFC through funds provided to the Sino-Germen CRC 110 "Symmetries and the Emergence of Structure in QCD", DFG Grant No. TRR 110 and NSFC Grant No. 11621131001.

[1] K. Hagiwara, C. B. Kim, and T. Yoshino, Nucl. Phys. **B177**, 461 (1981).
[2] A. Czarnecki and K. Melnikov, Phys. Lett. B **519**, 212 (2001).
[3] G. T. Bodwin, E. Braaten, and G. P. Lepage, Phys. Rev. D **51**, 1125 (1995); **55**, 5853(E) (1997).
[4] J. P. Lees *et al.* (*BABAR* Collaboration), Phys. Rev. D **81**, 052010 (2010).
[5] G. S. Adams *et al.* (CLEO Collaboration), Phys. Rev. Lett. **101**, 101801 (2008).
[6] C. C. Zhang *et al.* (BELL Collaboration), Phys. Rev. D **86**, 052002 (2012).
[7] M. Ablikim *et al.* (BESIII Collaboration), Phys. Rev. D **87**, 032003 (2013).
[8] J. J. Dudek and R. G. Edwards, Phys. Rev. Lett. **97**, 172001 (2006).
[9] T. Chen *et al.* (CLQCD Collaboration), Eur. Phys. J. C **76**, 358 (2016).
[10] Y. Chen *et al.* (CLQCD Collaboration), arXiv:2003.09817.
[11] F. Feng, Y. Jia, and W.-L. Sang, Phys. Rev. Lett. **119**, 252001 (2017).
[12] M. Tanabashi *et al.* (Particle Data Group), Phys. Rev. D **98**, 030001 (2018).
[13] X. Ji and C. Jung, Phys. Rev. Lett. **86**, 208 (2001).
[14] X. Ji and C. Jung, Phys. Rev. D **64**, 034506 (2001).
[15] J. J. Dudek, R. G. Edwards, and D. G. Richards, Phys. Rev. D **73**, 074507 (2006).
[16] X. Feng, S. Aoki, H. Fukaya, S. Hashimoto, T. Kaneko, J.-i. Noaki, and E. Shintani (JLQCD Collaboration), Phys. Rev. Lett. **109**, 182001 (2012).
[17] Y. Meng, C. Liu, and K. L. Zhang, arXiv:1910.11597v3.
[18] M. D. Schwartz, *Quantum Field Theory and the Standard Model* (Cambridge University Press, New York, 2014).
[19] R. Frezzotti, P. A. Grassi, S. Sint, and P. Weisz (ALPHA Collaboration), J. High Energy Phys. 08 (2001) 058, arXiv:hep-lat/0101001.
[20] P. Boucaud *et al.* (ETMC Collaboration), Phys. Lett. B **650**, 304 (2007).
[21] D. Becirevic and F. Sanfilippo, J. High Energy Phys. 01 (2013) 028.
[22] R. Frezzotti and G. Rossi, J. High Energy Phys. 10 (2004) 070.